J|A|C|S ARTICLES

Published on Web 06/24/2010

Direct Synthesis of Polymer Nanocapsules: Self-Assembly of Polymer Hollow Spheres through Irreversible Covalent Bond Formation

Dongwoo Kim,[†] Eunju Kim,[†] Jiyeong Lee,[†] Soonsang Hong,[†] Wokyung Sung,*[,‡] Namseok Lim,[§] Chan Gyung Park,[§] and Kimoon Kim*[,†]

National Creative Research Initiative Center for Smart Supramolecules, Department of Chemistry, Division of Advanced Materials Science, Department of Physics, and Department of Materials Science and Engineering, Pohang University of Science and Technology, San 31 Hyojadong, Pohang 790-784, Republic of Korea

Received May 8, 2010; E-mail: kkim@postech.ac.kr; wsung@postech.ac.kr

Abstract: A detailed study of the direct synthesis of polymer nanocapsules, which does not require any template, and core removal, is presented. Thiol−ene "click" reaction between a CB[6] derivative (**1**) with 12 allyloxy groups at the periphery and dithiols directly produced polymer nanocapsules with a highly stable structure and relatively narrow size distribution. Based on a number of observations including the intermediates detected by DLS, TEM, and SEM studies, a mechanism of the nanocapsule formation was proposed, which includes 2D oligomeric patches turning into a hollow sphere. A theoretical study supports that the formation of a hollow sphere from a disk-shaped intermediate can be thermodynamically favorable under certain conditions. In particular, the effects of various factors such as monomer concentration, reaction temperature, and medium on the formation of polymer nanocapsules have been investigated, which qualitatively agree with those predicted by our theoretical model. An interesting feature of the polymer nanocapsules was that the polymer shell made of a CB[6] derivative allows facile tailoring of its surface properties in a noncovalent and modular manner by virtue of the unique recognition properties of the accessible molecular cavities exposed on the surface. Furthermore, this approach appears to be applicable to any building unit with a flat core and multiple polymerizable groups at the periphery which can direct polymer growth in lateral directions. Other reactions, such as amide bond formation, can be used for the synthesis of polymer nanocapsules in this approach. This novel approach to polymer nanocapsules represents a rare example of self-assembly of molecular components into nanometer-scale objects with interesting structures, shapes, and morphology through irreversible covalent bond formation.

Introduction

Polymer nanocapsules are nanometer-sized hollow spheres whose shells are made of polymers. Virus capsids, which are made of multiple copies of identical protein subunits, are probably the best known example of naturally occurring polymer nanocapsules.[1] They not only are responsible for protecting genetic materials such as DNA and RNA kept inside but also play an important role in infecting host cells. Inspired by virus capsids, researchers have been studying synthetic polymer nanocapsules which also offer many interesting applications, including encapsulation, delivery, imaging, and catalysis.[2] Several methods to prepare synthetic polymer nanocapsules have been reported, which include template synthesis,[3] self-assembly,[4] emulsion polymerization,[5] and core removal of dendrimers.[6] Although each of these methods has its own merits and demerits, they all need either a preorganized structure or a template to shape a core−shell structure, and furthermore they require time-consuming and laborious multistep processes including removal of core or templates, repeated centrifugation or filtration, cross-linking of specially designed vesicular species, or separation of large quantities of surfactants.

In an investigation of the polymerization of (allyloxy)$_{12}$cucurbit[6]uril (**1**, Scheme 1), a synthetic host molecule having a cavity and 12 reactive allyloxy groups at the periphery, with dithiols via thiol−ene photopolymerization, we recently discovered the spontaneous formation of nanometer-sized polymer hollow spheres with a highly stable structure and relatively narrow size distribution.[7,8] This discovery prompted us to develop a one-pot, direct method for the synthesis of polymer nanocapsules without using a template or preorganized structure, and without removal of core or templates, which seems

[†] National Creative Research Initiative Center for Smart Supramolecules, Department of Chemistry, and Division of Advanced Materials Science.
[‡] Department of Physics.
[§] Department of Materials Science and Engineering.

(1) (a) Wikoff, W. R.; Liljas, L.; Duda, R. L.; Tsuruta, H.; Hendrix, R. W.; Johnson, J. E. *Science* **2000**, *289*, 2129–2133. (b) Johnson, J. E.; Chiu, W. *Curr. Opin. Struct. Biol.* **2000**, *10*, 229–236.

(2) (a) De Geest, B. G.; Sanders, N. N.; Sukhorukov, G. B.; Demeester, J.; De Smedt, S. C. *Chem. Soc. Rev.* **2007**, *36*, 636–649. (b) Meier, W. *Chem. Soc. Rev.* **2000**, *29*, 295–303. (c) Peyratout, C. S.; Dähne, L. *Angew. Chem., Int. Ed.* **2004**, *43*, 3762–3783. (d) Vriezema, D. M.; Aragonès, M. C.; Elemans, J. A. A. W.; Cornelissen, J. J. L. M.; Rowan, A. E.; Nolte, R. J. M. *Chem. Rev.* **2005**, *105*, 1445–1489. (e) Poe, S. L.; Kobašlija, M.; McQuade, D. T. *J. Am. Chem. Soc.* **2006**, *128*, 15586–15587. (f) Shchukin, D. G.; Sukhorukov, G. B. *Adv. Mater.* **2004**, *16*, 671–682.

 10.1021/ja1039242

Scheme 1. Synthesis of Polymer Nanocapsules **3** and Removal of the Disulfide Loops on the Surface To Produce Polymer Nanocapsules **3a′**

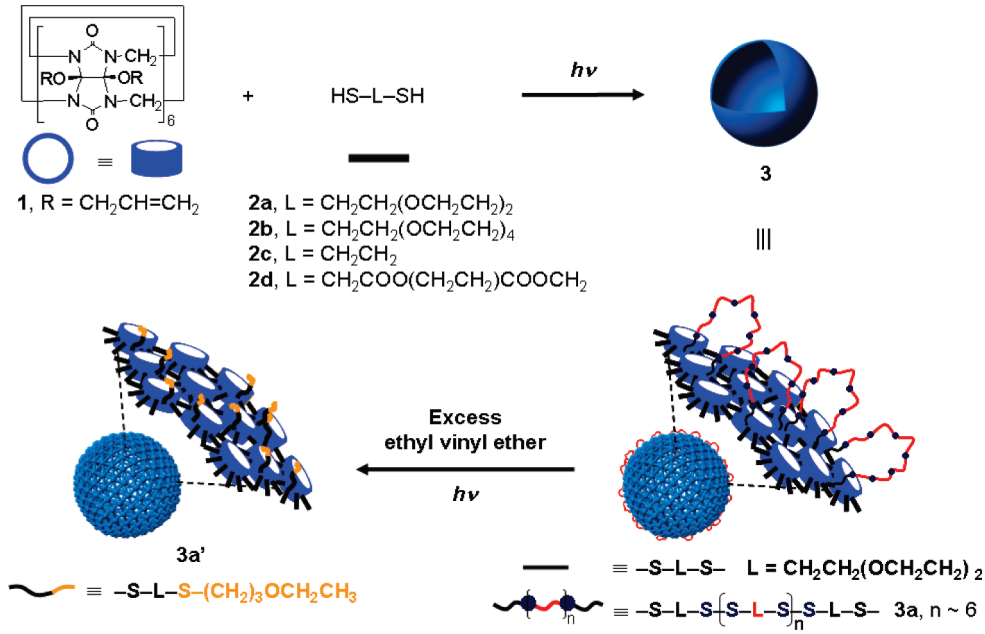

to be applicable to any monomers with a flat core and multiple polymerizable groups at the periphery. Following the initial communication,[7] we herein report the details of the experimental and theoretical study on the direct synthesis of the polymer nanocapsules made of **1** and dithiols, including the mechanism of formation of the polymer nanocapsules and the effects of monomer concentration, reaction temperature, and medium on the nanocapsule formation. This novel approach to polymer nanocapsules represents a rare example of self-assembly of molecular components into nanometer-scale objects with interesting structures, shapes, and morphology through irreversible covalent bond formation.

Results and Discussion

Synthesis and Characterization of Polymer Nanocapsules. Polymer nanocapsules were synthesized using photoinitiated thiol−ene "click" reaction[9] involving the reaction between $(allyloxy)_{12}$cucurbit[6]uril **1**, a rigid disk-shaped molecule with a cavity and 12 polymerizable allyl groups at the periphery,[10,11] and oligoethylene oxide or alkyl-based dithiols **2a**−**d**. The synthetic procedure is surprisingly simple. In a typical experiment, UV irradiation of a mixture of **1** and **2a** in a 1:48 ratio (allyloxy:thiol = 1:8) in methanol for 20 h, followed by dialysis against methanol, produced polymer nanocapsule **3a** in 87% yield based on **1** (Scheme 1).

The product was characterized by various spectroscopic, light scattering, and imaging techniques. The FT-IR spectrum of **3a** revealed two characteristic peaks of the cucurbit[6]uril (CB[6]) unit of **1** at 1765 and 1457 cm^{-1}, corresponding to the C=O and C−N stretching vibrations. In addition, the S−H stretching peak of **2a** at 2557 cm^{-1} and three peaks corresponding to the

(3) (a) Moughton, A. O.; O'Reilly, R. K. *J. Am. Chem. Soc.* **2008**, *130*, 8714–8725. (b) Liu, X.; Basu, A. *J. Am. Chem. Soc.* **2009**, *131*, 5718–5719. (c) Cavalieri, F.; Postma, A.; Lee, L.; Caruso, F. *ACS Nano* **2009**, *3*, 234–240. (d) Schwiertz, J.; Meyer-Zaika, W.; Ruiz-Gonzalez, L.; Gonzlez-Calbet, J. M.; Vallet-Regí, M.; Epple, M. *J. Mater. Chem.* **2008**, *18*, 3831–3834. (e) Choi, W. S.; Park, J.-H.; Koo, H. Y.; Kim, J.-Y.; Cho, B. K.; Kim, D.-Y. *Angew. Chem., Int. Ed.* **2005**, *44*, 1096–1101. (f) Blomberg, S.; Ostberg, S.; Harth, E.; Bosman, A. W.; Horn, B. V.; Hawker, C. J. *J. Polym. Sci. Part A* **2002**, *40*, 1309–1320. (g) Gittins, D. I.; Caruso, F. *Adv. Mater.* **2000**, *12*, 1947–1949. (h) Sun, L.; Crooksa, R. M.; Chechik, V. *Chem. Commun.* **2001**, 359–360. (i) Donath, E.; Sukhorukov, G. B.; Caruso, F.; Davis, S. A.; Möhwald, H. *Angew. Chem., Int. Ed.* **1998**, *37*, 2201–2205.
(4) (a) Wang, Y.; Angelatos, A. S.; Caruso, F. *Chem. Mater.* **2008**, *20*, 848–858. (b) Dong, W.-F.; Kishimura, A.; Anraku, Y.; Chuanoi, S.; Kataoka, K. *J. Am. Chem. Soc.* **2009**, *131*, 3804–3805. (c) Xu, P.; Li, S.-Y.; Li, Q.; Van Kirk, E. A.; Ren, J.; Murdoch, W. J.; Zhang, Z.; Radosz, M.; Shen, Y. *Angew. Chem., Int. Ed.* **2008**, *120*, 1280–1284. (d) Scott, C.; Wu, D.; Ho, C.-C.; Co, C. C. *J. Am. Chem. Soc.* **2005**, *127*, 4160–4161. (e) Hu, Y.; Jiang, X.; Ding, Y.; Chen, Q.; Yang, C. *Adv. Mater.* **2004**, *16*, 933–937. (f) Jung, H. M.; Price, K. E.; McQuade, D. T. *J. Am. Chem. Soc.* **2003**, *125*, 5351–5355. (g) Breitenkamp, K.; Emrick, T. *J. Am. Chem. Soc.* **2003**, *125*, 12070–12071. (h) Stewart, S.; Liu, G. *Chem. Mater.* **1999**, *11*, 1048–1054. (i) Huang, H.; Remsen, E. E.; Kowalewski, T.; Wooley, K. L. *J. Am. Chem. Soc.* **1999**, *121*, 3805–3806. (j) Dinsmore, A. D.; Hsu, M. F.; Nikolaides, M. G.; Marquez, M.; Bausch, A. R.; Weitz1, D. A. *Science* **2002**, *298*, 1006–1009.
(5) (a) Lu, F.; Luo, Y.; Li, B.; Zhao, Q.; Schork, F. J. *Macromolecules* **2010**, *43*, 568–571. (b) Okubo, M.; Konishi, Y.; Minami, H. *Colloid Polym. Sci.* **1998**, *276*, 638–642. (c) Sarkar, D.; El-Khoury, J.; Lopina, S. T.; Hu, J. *Macromolecules* **2005**, *38*, 8603–8605. (d) Jang, J.; Ha, H. *Langmuir* **2002**, *18*, 5613–5618.
(6) (a) Zimmerman, S. C.; Wendland, M. S.; Rakow, N. A.; Zharov, I.; Suslick, K. S. *Nature* **2002**, *418*, 399–403. (b) Wendland, M. S.; Zimmerman, S. C. *J. Am. Chem. Soc.* **1999**, *121*, 1389.
(7) Kim, K.; et al. *Angew. Chem., Int. Ed.* **2007**, *46*, 3471–3474.
(8) Kuykendall, D. W.; Zimmerman, S. C. *Nat. Nanotechnol.* **2007**, *2*, 201.
(9) (a) Dondoni, A. *Angew. Chem., Int. Ed.* **2008**, *47*, 8995. (b) Hoyle, C. E.; Bowman, C. N. *Angew. Chem., Int. Ed.* **2010**, *49*, 1540–1573. (c) Killops, K. L.; Campos, L. M.; Hawker, C. J. *J. Am. Chem. Soc.* **2008**, *130*, 5062–5064. (d) Cramer, N. B.; Reddy, S. K.; Cole, M.; Hoyle, C.; Bowman, C. N. *J. Polym. Sci. Part A* **2004**, *42*, 5817–5826.
(10) Jon, S. Y.; Selvapalam, N.; Oh, D. H.; Kang, J.-K.; Kim, S.-Y.; Jeon, Y. J.; Lee, J. W.; Kim, K. *J. Am. Chem. Soc.* **2003**, *125*, 10186–10187.
(11) For reviews on the CB[*n*] chemistry, see: (a) Mock, W. L. In *Comprehensive Supramolecular Chemistry*; Vögtle, F., Ed.; Pergamon: Oxford, 1996; Vol. 2, p 477. (b) Lee, J. W.; Samal, S.; Selvapalam, N.; Kim, H.-J.; Kim, K. *Acc. Chem. Res.* **2003**, *36*, 621–630. (c) Lagona, J.; Mukhopadhyay, P.; Chakrabarti, S.; Isaacs, L. *Angew. Chem., Int. Ed.* **2005**, *44*, 4844–4870. (d) Kim, K.; Selvapalam, N.; Ko, Y. H.; Park, K. M.; Kim, D.; Kim, J. *Chem. Soc. Rev.* **2007**, *36*, 267–279.

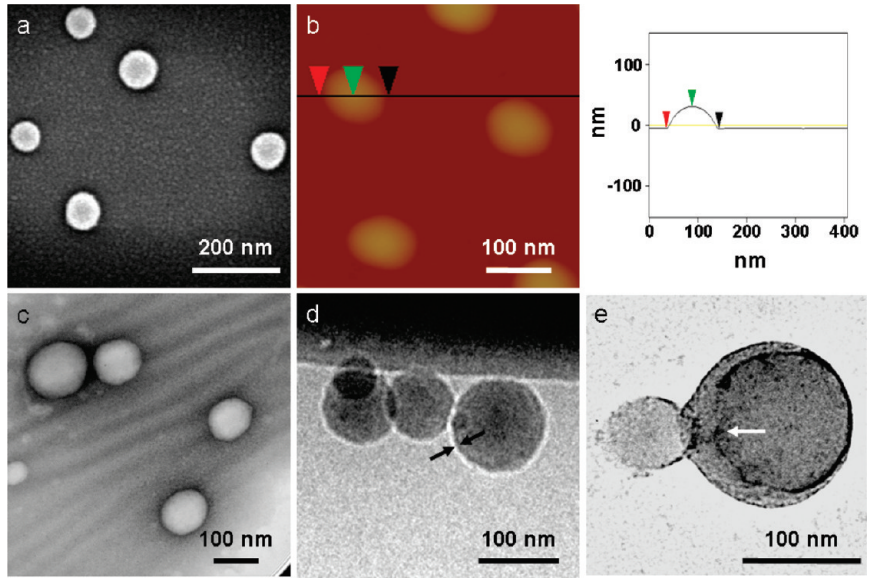

Figure 1. (a) SEM image, (b) AFM image (left) and height profile (right) along the line in the AFM image, (c) HR-TEM image, and (d) cryo-TEM image of polymer nanocapsules **3a**. (e) HR-TEM image of **3a** showing a ruptured wall (indicated by an arrow).

allyl groups of **1** at 1647, 3017, and 3084 cm^{-1} disappeared completely (Figure S1, Supporting Information). The lack of the olefin peaks at 120 and 136 ppm and the presence of a thioether peak at 35 ppm in the solid-state ^{13}C NMR spectrum of **3a** confirmed the complete consumption of the allyl groups of **1** and formation of new thioether linkages (Figure S2, Supporting Information).

The nanometer-sized colloidal particle nature of **3a** (average diameter of 110 ± 30 nm) was first revealed by dynamic light scattering (DLS) studies. Scanning electron microscopy (SEM) of **3a** confirmed the spherical-shaped product (Figure 1a), but the size of the dried sample was somewhat smaller (average diameter of 70 ± 20 nm) than that in solution estimated by DLS. Tapping-mode atomic force microscopy (AFM) of **3a** (Figure 1b) showed flattened spheres with an average diameter of 107 ± 10 nm and a height of 40 ± 6 nm. Most importantly, however, a combination of dynamic and static light scattering studies showed that the radius of gyration (R_g = 60.2 nm) and hydrodynamic radius (R_h = 57.3 nm) are almost the same ($\rho(R_g/R_h) = 1.05$), indicating the hollow-sphere nature of **3a**,[12] which was confirmed by high-resolution and cryo transmission electron microscopy (TEM) studies, revealing a hollow interior surrounded by a thin shell with an average thickness of 2.1 ± 0.3 nm (Figure 1c,d). Considering that the height of CB[6] is approximately 1 nm, this result suggested that the nanocapsule shell is only one or two monomers thick, consistent with the results of the titration experiment to determine the accessible CB[6] cavities on the surface of the polymer nanocapsule (see below). One interesting observation is that, unlike previous known polymer nanocapsules, polymer nanocapsule **3a** is robust enough to maintain a spherical shape even under SEM and TEM conditions. The robust structure of the polymer nanocapsule often made the investigation of its inner structure difficult. However, several freeze−thaw cycles using liquid nitrogen, carried out on polymer nanocapsule **3a** dispersed in 1−10% methanol in water, produced a significant amount of ruptured nanocapsules (Figure 1e). Repeated expansion and shrinkage of the water entrapped inside the capsules seems to cause the breakage of the weakest part of the capsule wall, which allowed us to easily characterize the hollow nature of the polymer nanocapsule dispersed in aqueous solution.

Having established the hollow sphere nature of **3a**, we investigated the chemical composition and structure of the shell of polymer nanocapsule **3a**. Since **1** has 24 nitrogen atoms but no sulfur atom, whereas **2a** contains two sulfur atoms but no nitrogen atom, elemental analysis (especially the N/S ratio) of **3a** provided a clue to the composition and structure of the polymer network constituting the nanocapsule shell. Elemental analysis showed that the ratio of **1** and **2a** incorporated into **3a** is 1:15.5, which decreased to 1:7.4 after treating **3a** with excess ethyl vinyl ether under UV light (**3a′**). These results suggested that, upon completion of the reaction between **1** and **2a**, approximately 9 of the 12 allyl groups of **1** form thioether bridges with a composition of $-O(CH_2)_3S-L-S(CH_2)_3O-$ (L = $CH_2CH_2(OCH_2CH_2)_2$), linking neighboring CB[6] units to produce a two-dimensional (2D) polymer network that constitutes the shell of the nanocapsule, and the remaining three allyl groups form disulfide loops with an average composition of $-O(CH_2)_3S-L-S-(S-L-S)_n-S-L-S(CH_2)_3O-$ ($n \approx 6$), protruding on the nanocapsule surface as illustrated here. Such a highly cross-linked polymer network makes the polymer nanocapsules exceptionally robust even though the shell is only one or two monomers thick. Furthermore, the extra disulfide loops, which can be removed by treatment with excess ethyl vinyl ether (Scheme 1), reinforce the thin shell of the nanocapsule to make the polymer nanocapsule hard, highly stable, and little responsive to changes in medium. The polymer nanocapsule **3a′** obtained by the ethyl vinyl ether treatment is more responsive to changes in environment, which allowed us to control the permeability of the shell by changing media, as reported recently.[13]

Monitoring the Formation of Polymer Nanocapsules. To understand the mechanism of the formation of the polymer nanocapsule, we monitored the photopolymerization of **1** and

(12) Nardin, C.; Hirt, T.; Leukel, J.; Meier, W. *Langmuir* **2000**, *16*, 1035–1041.

(13) Kim, E.; Lee, J.; Kim, D.; Lee, K. E.; Han, S. S.; Lim, N.; Kang, J.; Park, C. G.; Kim, K. *Chem. Commun.* **2009**, 1472–1474.

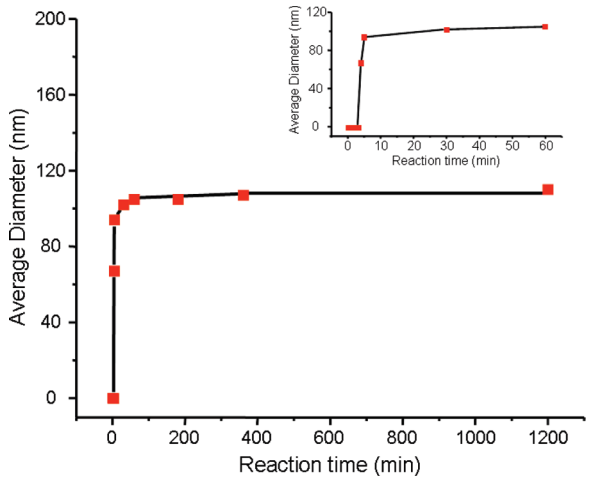

Figure 2. Change in the average size of the product (observed by DLS) during the formation of polymer nanocapsule **3a** from **1** and **2a** (1:48) (inset: size change during the first 60 min).

2a (1:48) in methanol by DLS, FT-IR spectroscopy, and elemental analysis. Before UV irradiation, no preorganized structure in the reaction mixture was observed by DLS. However, after ~4 min of the reaction, particles with an average size of 70 nm appeared abruptly. The particle size quickly reached ~100 nm within 10 min and finally reached 105 nm in 20 h (Figure 2). The FT-IR spectrum of the product isolated after 3 h of reaction showed the presence of the C=C stretching peak of unreacted allyl groups at 1647 cm^{-1}, which slowly disappeared over the next several hours (Figure S3, Supporting Information). Elemental analysis of the isolated product indicated that the percentage of **1** incorporated into the product was ~60% after 3 h of the reaction and increased to 87% by the end of the reaction (20 h). Furthermore, the ratio of **1** and **2a** incorporated into the product was ~1:8 after 3 h of the reaction, which slowly increased to ~1:16 at the end of the reaction.

We also monitored the same reaction in *chloroform* by DLS, in which a much larger polymer nanocapsule was produced compared to that in methanol. The reaction profile (particle size vs reaction time) monitored by DLS was pretty much the same as that in methanol (Figure S4, Supporting Information). In this case, however, particles with an average size of 560 nm suddenly appeared after ~3 min of the reaction. The particle size increased to 770 nm within 30 min and finally reached 820 nm after 20 h. The production of larger polymer nanocapsules in chloroform allowed us to characterize the product at each stage of the polymerization by TEM and SEM (Figures 3 and S5, Supporting Information). At the very early stage of the reaction (1 min), thin polymer patches with a size ranging from 100 to 120 nm were detected (Figure 3a). Interestingly, they have many holes as large as 20 nm. Much larger patches (400−500 nm) were observed after 2 min (Figure 3b), and half-shell-like polymer species of 400−500 nm were observed after 5 min (Figure 3c). After 1 h, hollow capsules of 400−600 nm (with imperfection in some cases) were seen (Figure 3d), and matured polymer nanocapsules with an average size of ~600 nm were observed afterward (10 and 20 h) (Figure 3e,f).

Proposed Mechanism of the Nanocapsule Formation. On the basis of the above observations and general features of the thiol−ene photopolymerization, which is known to follow a free-radical step growth mechanism,[9] we propose a mechanism for the formation of the polymer nanocapsule as shown in Figure 4. At the early stage of the reaction, disk-shaped monomers (**1**) with multiple polymerizable groups at the periphery react with dithiyl radicals initially generated by UV irradiation to form dimers and trimers linked by thioether linkages, which further react with each other to grow into 2D oligomeric patches, as a result of the edge-to-edge connection of the monomers (**1**) through multiple thioether bridges. Such 2D oligomeric patches, especially the ones produced at the early stage of the reaction, may have some "holes" (imperfection sites), as observed by TEM (Figure 3a). A 2D oligomeric patch of a certain size starts to bend to reduce its total energy, and further reaction between the curved oligomeric patches generates a loosely cross-linked hollow sphere. Some of the remaining allyl groups participate in additional thioether bridge formation between neighboring

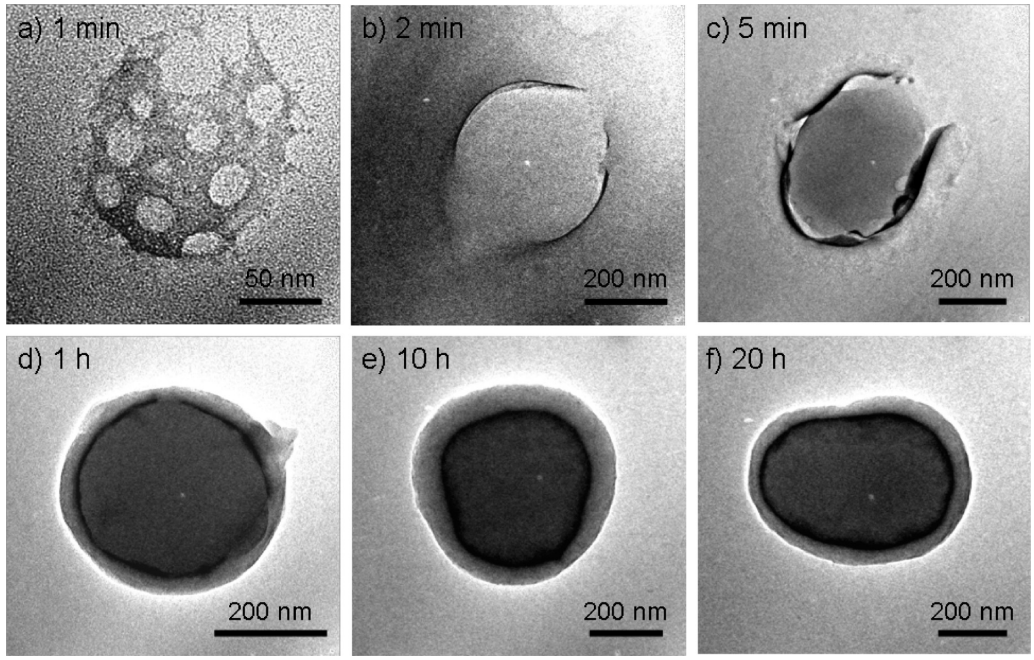

Figure 3. HR-TEM images at each stage of the polymerization of **1** and **2a** (1:6) in chloroform.

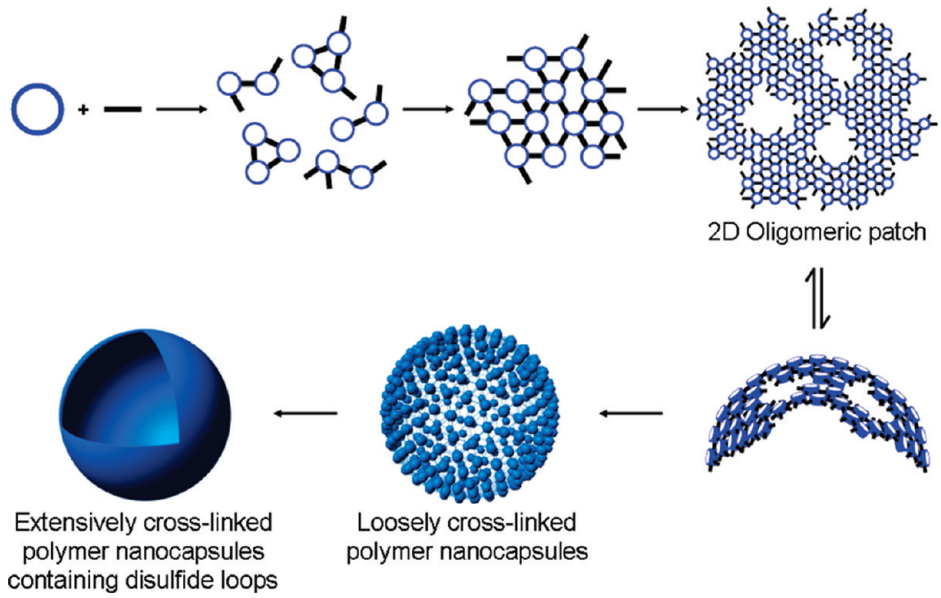

Figure 4. Proposed mechanism of the polymer nanocapsule formation.

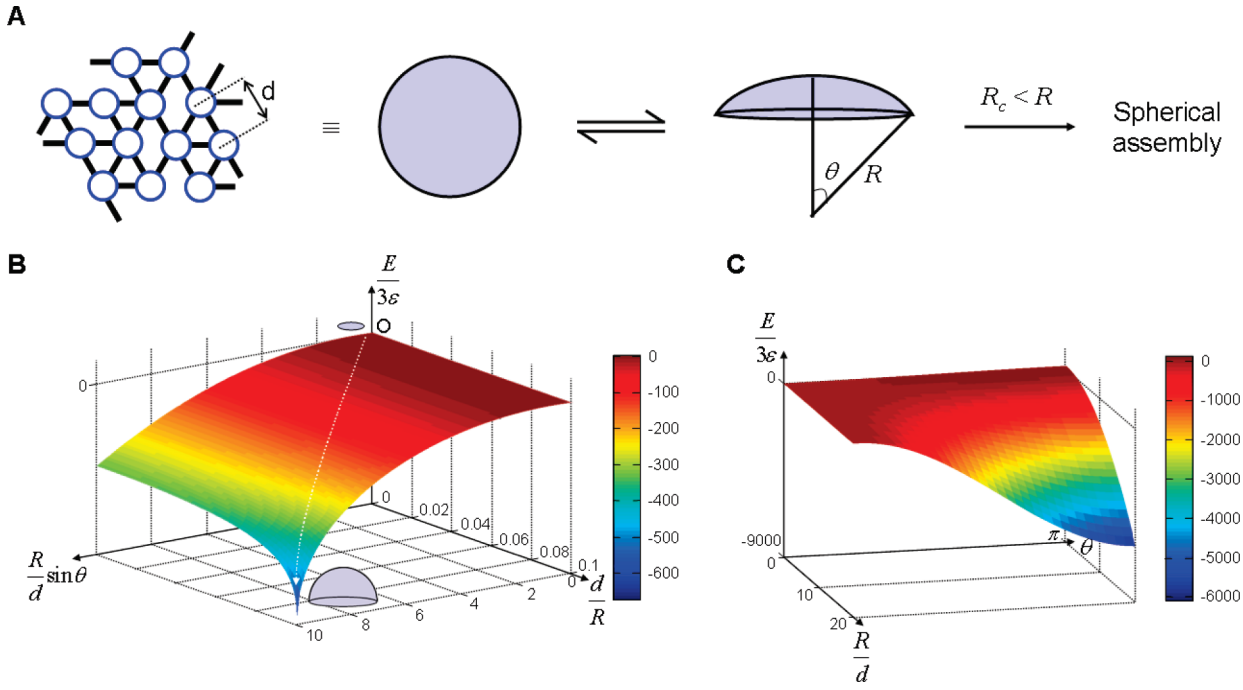

Figure 5. (a) Theoretical model for the conversion of a disk (representing a 2D oligomeric patch) into a cap and then a hollow sphere. (b) Energy profile ($E/3\varepsilon$) of a cap as a function of $R \sin\theta/d$ and d/R, assuming that $\kappa = 15\varepsilon$ and $f = 6$. (c) Energy profile ($E/3\varepsilon$) of a cap as a function of θ and R/d, using the same parameters as above and $R_c = 2.8d$.

CB[6] units in the shell to produce a highly cross-linked polymer nanocapsule, while the rest of the allyl groups lead to the formation of disulfide loops protruding on the nanocapsule surface (Scheme 1).

The proposed mechanism is similar to the well-accepted mechanism of the formation of vesicles made of lipids, in which a 2D planar bilayer structure is assumed to be involved before it turns into a vesicle.[14] The major difference is that covalent bonds are irreversibly formed between the building units in the lateral directions in the present system, while reversible noncovalent interactions are involved along lateral directions in vesicles.

Theoretical Studies on the Formation of Polymer Nanocapsules. For a better understanding of the polymer nanocapsule formation, including the energetics and size distribution of nanocapsules, we have developed a theoretical model. In any process of self-assembly approaching equilibrium, the system tends to reduce the free energy given certain constraints. We postulate that a hollow sphere can form spontaneously from a disk as below.

Assume that a disk attains a curvature and transforms to a spherical cap with a radius of curvature R and θ (Figure 5a) as an intermediate during 2D polymerization. The number of monomers in the cap is approximately $2\pi R^2(1 - \cos\theta)/\pi(d/$

$2)^2$. Here d is the distance between two adjacent monomer units in the aggregate. Compared with an unbound monomer, a bound monomer in the aggregate has lower energy, $-f\varepsilon/2$, where ε is the bond energy per linkage and f is the number of such linkages per monomer. Here we consider an ideal case where every monomer in the aggregate is fully bonded (hexagonally in our case) with neighboring monomers, i.e., $f = 6$. The qualitative results obtained here will remain valid for non-ideal cases where the bonding is not complete. The surface energy is then given by

$$-\frac{f}{2}\varepsilon\frac{2\pi R^2}{\pi(d/2)^2}(1 - \cos\theta) \tag{1}$$

On the rim of the cap such bonds are absent, so there is an energy cost to expose the rim by the amount $3\varepsilon(2\pi R/d)\sin\theta$. In addition, a bending energy is required to create the curvature, which can be written as the surface integral $(1/2)\kappa\int dA(2/R)^2 = 4\pi\kappa(1 - \cos\theta)$, where κ is the bending rigidity. The total energy change for forming the cap, then, is

$$E = -3\varepsilon\left[\frac{8R^2}{d^2}(1 - \cos\theta) - \frac{2\pi R}{d}\sin\theta\right] + 4\pi\kappa(1 - \cos\theta) \tag{2}$$

To support our assumption on spontaneous curvature formation, we investigate eq 2, rewritten as below, for $0 < \theta < \pi/2$, namely the first half-stage of the capsule formation,

$$\frac{E}{3\varepsilon} = -\frac{8}{y^2}(1 - \sqrt{1 - (xy)^2}) + 2\pi x + \frac{4\pi\kappa}{3\varepsilon}(1 - \sqrt{1 - (xy)^2}) \tag{3}$$

where $x = (R/d)\sin\theta$ and $y = d/R$ are the rescaled cap radius and curvature. As depicted in Figure 5b, the equation shows that an initial patch of *flat* disk with a small radius $a = R\theta$ (with $R \rightarrow \infty$, $\theta \rightarrow 0$), corresponding to a state near the origin O, is unstable with respect to transition to the states of finite curvature, culminating in a hollow hemisphere ($x = R/d$, $y = d/R$) at $= \pi/2$. For the case where $\kappa = 15\varepsilon$, its radius R is about $10d$. The most probable pathway of the transition is indicated by a dotted line in Figure 5b.

Figure 5c is a generic shape of the energy landscape in coordinates R and θ. The equation predicts and the figure also shows that, for R larger than the critical value $R_c = d(\pi\kappa/6\varepsilon)^{1/2}$, the energy landscape is downhill at $\theta = \pi$; i.e., at the moment of the complete sphere formation, where the energy attains the minimum,

$$E_m = -\frac{48\varepsilon R^2}{d^2} + 8\pi\kappa \tag{4}$$

which falls more steeply far below zero for a larger R! This means that, if the surface energy gain dominates over the bending energy cost, a hollow sphere of a radius larger than the critical value R_c can spontaneously and rapidly form. Otherwise, an energy barrier to sphere formation appears to be too high to be overcome by thermal fluctuation.

Now let us consider the size distribution of the hollow spheres formed in the self-assembly process. Although the energy dictates fewer, larger hollow spheres to form as suggested by eq 4, the entropy favors more and smaller spheres. To obtain an equilibrium size distribution of the spheres that minimizes the free energy of the system, we adapt the general theory of self-assembly to our system.[14]

The chemical potential μ_N of a monomer in an aggregate (or a hollow sphere) composed of N monomers is given by

$$\mu_N = \mu_N^\circ + \frac{kT}{N}\ln\frac{X_N}{N} \tag{5}$$

where X_N is the monomer concentration in N-aggregates in volume fraction and k is the Boltzmann constant. While μ°_N is the energy contribution to the chemical potential, the second term of eq 5 represents the entropy contribution of the aggregates regarded as an ideal gas. In chemical equilibrium of a monomer in N-aggregates with an unbound monomer, $\mu_1 = \mu_N$, which yields

$$X_N = N\{X_1\exp[(\mu_1^\circ - \mu_N^\circ)/kT]\}^N \tag{6}$$

We are interested in finding concentration of the aggregates $C_N = X_N/N$ in terms of total monomer concentration $C = \sum_{N=N_c}^{\infty} X_N$, where N_c is the critical aggregate number, defined by $N_c = 4\pi R_c^2/\pi(d/2)^2$.

We first note that, from eq 4,

$$\mu_N^\circ = \mu_\infty^\circ + \frac{8\pi\kappa}{N} \tag{7}$$

where μ°_∞ is the binding energy per monomer in an infinite aggregate (a hollow sphere of infinite radius). Also we have

$$\mu_\infty^\circ - \mu_1^\circ = -3\varepsilon \tag{8}$$

where ε is the bond energy per linkage. From eq 6, then, we have for N larger than N_c,

$$X_N = N[X_1\, e^{\lambda}\, e^{-\gamma/N}]^N \tag{9}$$

where $\lambda = 3\beta\varepsilon$, $\gamma = 8\pi\beta\kappa$, and $\beta = 1/kT$.

We consider the case where X_1, the concentration of monomer in unbound state, is lower than $e^{-\lambda}$ so that large aggregates can form. The total concentration is

$$C = \sum_{N=N_c}^{\infty} X_N = \sum_{N=N_c}^{\infty} Ny^N\, e^{-\gamma} = \frac{y + N_c y^{N_c-1} - N_c y^{N_c}}{(1 - y)^2}\, e^{-\gamma}$$

where $y = X_1\, e^{\lambda}$. Since $N_c \gg 1$, $y^{N_c} \ll 1$, so that we have

$$C = \frac{X_1\, e^{\lambda}\, e^{-\gamma}}{(1 - X_1\, e^{\lambda})^2} \tag{10}$$

From eq 10 we obtain

$$X_1 = \frac{2C + e^{-\gamma} - \sqrt{4C\, e^{-\gamma} + e^{-2\gamma}}}{2C\, e^{\lambda}} \tag{11}$$

We consider the case where $C \gg e^{-\gamma}$ as well as $C \gg e^{-\lambda}$. Then we obtain

$$X_1 \approx e^{-\lambda}\left[1 - \frac{1}{\sqrt{C\, e^{\gamma}}}\right] \tag{12}$$

$$X_N = N\left(1 - \frac{1}{\sqrt{C\,e^{\gamma}}}\right)^N e^{-\gamma} \approx N\,e^{-(N/\sqrt{C\,e^{\gamma}}+\gamma)} \quad (13)$$

$$C_N = \frac{X_N}{N} = e^{-(N/\sqrt{C\,e^{\gamma}}+\gamma)} \quad (14)$$

To find the radius distribution $P(R)$ of the spheres rather than its concentration C_N, we note the number of spheres within a small range of the aggregate number and radius, ΔN and ΔR, respectively, given by $P(R)\Delta R \propto C_N \Delta N$, from which we obtain

$$P(R) \propto C_N \frac{dN}{dR} \quad (15)$$

Since $N = 16\pi R^2/\pi d^2$, we find

$$P(R) = 2\alpha R\, e^{-\alpha(R^2 - R_c^2)} \quad (16)$$

where $\alpha = (16/d^2)(C\,e^{\gamma})^{-1/2}$.

The distribution function eq 16 is in the form of a weighted Gaussian. Since $\alpha R_c^2 \ll 1$ in our case, we find that the average of the radius and standard deviation are respectively

$$\langle R \rangle = \int dR\, RP(R) = \frac{\sqrt{\pi}}{8}\, dC^{1/4}\, e^{2\pi\kappa/kT} \quad (17)$$

$$[\langle R^2 \rangle - \langle R \rangle^2]^{1/2} = \frac{1}{4}\sqrt{\left(1 - \frac{\pi}{4}\right)}\, dC^{1/4}\, e^{2\pi\kappa/kT} \quad (18)$$

both of which are of the same order of magnitude.

Equation 17 suggests that changes in the distance between neighboring monomers d and the bending rigidity κ via modulation of polymer stiffness and solvents affect the average size in a very appreciable manner, which is qualitatively in good agreement with the experimental results as described below.

Effect of Monomer Ratio on the Formation of Polymer Nanocapsules. In step-growth polymerization, the molar ratio of monomers affects the molecular weight and polydispersity of the resulting polymeric materials.[15] Similarly, the initial molar ratio of **1** and **2a** significantly affected the average diameter and size distribution of polymer nanocapsule **3a**, as confirmed by DLS studies. The average diameter of polymer nanocapsule **3a** was measured by DLS as a function of the number of equivalents of **2a** (Figure 6a) with respect to **1**. Essentially no polymerization of **1** was observed in the absence of **2a** with UV irradiation, as confirmed by ^{1}H NMR studies. The average diameter and its variance of the nanocapsule produced gradually increased with increasing number of equivalents of **2a** used. This observation is qualitatively in good agreement with what our theoretical model predicts. As the number of equivalents of **2a** increases, the average number of the thioether linkages connecting adjacent CB[6] units increases. As a result, the enhanced bending rigidity (κ) increases the average size and its variance of the nanocapsule in accordance with eqs 17 and 18 of our theoretical model.

Effect of Reaction Temperature on the Formation of Polymer Nanocapsules. When the reaction temperature decreased, the average diameter of the polymer nanocapsule decreased (Figure 6b), as indicated by DLS studies. For example, the photochemical reaction of **1** and **2a** in methanol at 38 °C (the temperature inside the photochemical reactor) produced polymer nanocapsule **3a** with an average diameter of 110 ± 30 nm, whereas the photoreaction at 8 °C yielded the polymer nanocapsule with an average diameter of 70 ± 20 nm. As the number of equivalents of **2a** increased in the reaction mixture, their average diameter prepared at 8 °C also increased, following the same trend observed at 38 °C. According to our theoretical model, the average diameter of the nanocapsule is proportional to $\exp(2\pi\kappa/kT)$, which predicts that the average diameter of the nanocapsule produced at 8 °C would be somewhat larger than that at room temperature, if the bending rigidity (κ) of the reaction intermediate (2D oligomeric patch) is the same. However, the reaction is slower at a lower temperature, at which the reaction intermediate should have a smaller number of dithioether linkages between the CB[6] units, leading to lower bending rigidity compared to that at a higher temperature. The experimental results suggest that the temperature-dependent change in the bending rigidity is larger than the temperature change itself so that the decrease in the reaction temperature results in a smaller κ/T value, leading to the decrease in the size of the nanocapsule.

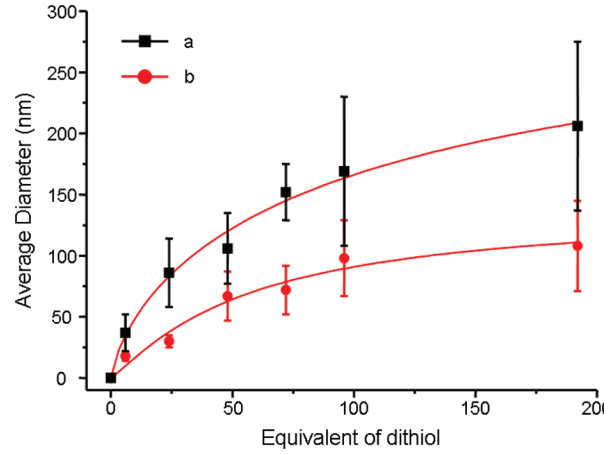

Figure 6. Average diameter of polymer nanocapsule **3a** synthesized at (a) 38 and (b) 8 °C as a function of the number of equivalents of dithiol **2a** used. The bar indicates the variance of the size.

Effect of Monomer Concentration on the Formation of Polymer Nanocapsules. When we increased the concentrations of the reactants **1** and **2a** in the reaction mixture while keeping the ratio of **1** to **2a** constant (1:48), the average diameter of the nanocapsules increased with increasing concentrations of the monomers, as indicated by DLS studies. For example, the photoreaction carried out with three different concentrations of **1**, 5×10^{-3}, 5×10^{-4}, and 5×10^{-5} M, produced the polymer nanocapsule with an average diameter of 170 ± 40, 110 ± 30, and 70 ± 10 nm, respectively. However, the reaction carried out with a concentration of **1** below 5×10^{-6} M generated only ill-defined polymer aggregates, indicating that there is a critical concentration of the monomer for the formation of the nanocapsule. The results indicated that the average size of the polymer nanocapsules seems to be proportional to the one-fifth power of the concentration of **1** (Figure 7), which may be comparable to that predicted by our theoretical model ($C^{1/4}$, eq 17). However, the large size distribution of the nanocapsule observed experimentally makes a precise comparison between the theory and experiment difficult.

Effect of Reaction Medium on the Formation of Polymer Nanocapsules. Reaction media play an important role in the formation of the polymer nanocapsule and controlling its size. For example, the photopolymerization of **1** and **2a** in acetonitrile

(14) Israelachvili, J. N. *Intermolecular & Surface Forces*; Academic Press: London, 1992.
(15) Odian, G. *Principles of Polymerization*; John Wiley and Sons: New York, 1991.

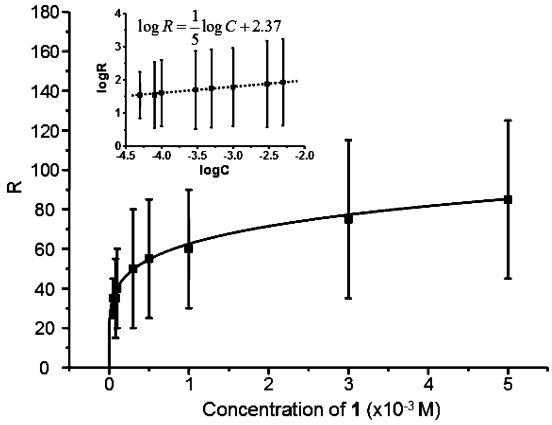

Figure 7. Radius of polymer nanocapsule **3a** measured by DLS studies as a function of the concentration of monomer **1** and the corresponding log−log plot (inset).

(Figure 8a) and chloroform (Figure 8b) produced the polymer nanocapsule with an average diameter of 150 ± 50 and 600 ± 100 nm (measured by SEM), respectively. In general, better solvents seemed to produce larger polymer nanocapsules. It is well known that polymer chains in good solvents are expanded to maximize the polymer chain−solvent contacts, whereas the chain segments in poor solvent stay close to each other.[16] Similarly, a two-dimensional polymer is known to be extended in good solvent and crumpled in poor solvent. Perhaps in poor solvents such as methanol, the strong tendency to reduce the surface energy (first term in eq 2) of a 2D oligomeric patch and energy cost to expose its rim to solvent (second term in eq 2) drives the system to generate smaller-sized nanocapsules compared to those in good solvents such as chloroform.

Effect of the Length of Dithiol on the Size of Polymer Nanocapsules. To understand the effect of the length of dithiol on the size of the nanocapsule produced, we used a longer dithiol **2b** and shorter dithiol **2c** (Scheme 1) instead of **2a** in the synthesis of the nanocapsule. DLS studies revealed that the longer dithiol **2b** produces a larger nanocapsule (**3b**, average diameter 140 ± 40 nm), whereas the shorter dithiol **2c** yields a smaller nanocapsule (**3c**, average diameter 50 ± 10 nm) under the same conditions (Figure 9). In general, the longer the dithiol was used, the larger the nanocapsule produced, which is consistent with the theory. These results also suggest that the size of the polymer capsules can be systematically controlled by the length of dithiol used.

Many functional groups can be incorporated into the shell of polymer nanocapsules by using dithiols containing such functional groups at the middle of the linkers in the nanocapsule synthesis, as long as they do not interfere with the production of 2D oligomeric patches through the thiol−ene click reaction. For example, the reaction of **1** with dithiol **2d** containing ester groups at the middle of the linker produced polymer nanocapsule **3d** (average diameter 120 ± 50 nm) with a cross-linked polymer network containing ester groups, which are breakable in the presence of acid stimuli. Similarly, we successfully introduced azobenzene units into the 2D polymer network of a photosensitive polymer nanocapsule, the details of which will be reported in a separate publication.

Effect of Additives on the Formation of Polymer Nanocapsules. The average size of the polymer nanocapsule can be controlled by addition of a small molecule in the reaction medium, which can interact with the monomers, especially **1**, since it has a CB[6] unit with a hydrophobic cavity and two identical polar carbonyl-laced portals, which is known to bind various ions and molecules via noncovalent interactions such as hydrogen-bonding and charge−dipole interaction.[11] For example, the photoreaction of **1** and **2a** (**1**:**2a** = 1:6) in methanol in the presence of 4-amino-1-butanol, which is known to bind to CB[6] with a moderate affinity ($K \approx 10^3$),[17] produced polymer nanocapsule **3a**, the average size of which is larger than that produced in the absence of the additive, as confirmed by SEM studies (Figure S6, Supporting Information). The average diameter of the nanocapsule increased with increasing number of equivalents of 4-amino-1-butanol added up to 6 equiv. These results clearly indicate that the binding of 4-amino-1-butanol to the CB[6] unit of **1** affected the behavior of the 2D oligomeric intermediates produced, and ultimately the size and size distribution of the polymer nanocapsule.

Encapsulation of Guest Molecules and Size-Selective Permeability of Polymer Nanocapsules. We can entrap large guest molecules inside the polymer nanocapsules by carrying out the nanocapsule formation reaction in the presence of the guest molecules. For example, UV irradiation of a mixture of **1** and **2a** (1:48) in methanol in the presence of carboxyfluorescein (CF) followed by dialysis produced a polymer nanocapsule encapsulating carboxyfluorescein (CF@**3a**) with an average diameter of 160 ± 40 nm, as confirmed by DLS and SEM studies.[7] A red shift (∼30 nm) of the emission band of CF along with the color change from yellow to red confirmed the successful encapsulation of the fluorescent dye. Further dialysis for days did not change the position and intensity of the emission band, supporting the trapping of the guest molecule.[7]

Similarly, fluorescent dye rhodamine 6G (Rh6G) was entrapped inside the polymer nanocapsule **3a** (average diameter 600 ± 150 nm, measured by SEM) by photopolymerization of **1** and **2a** (1:6) in chloroform in the presence of Rh6G. A red shift (∼7 nm) of the emission band of Rh6G was observed after encapsulation. The dye-encapsulating polymer nanocapsule (Rh6G@**3a**) was large enough to be observed by confocal laser scanning microscopy (Figure 10b), which will be further discussed below.

To check the permeability of the nanocapsule shell, we added an acid or methyl viologen to a dispersion of CF@**3a** and monitored the emission of the encapsulated dye molecule as a function of time. Addition of a drop of 0.5 M HCl to a dispersion of CF@**3a** instantly turned off the emission of CF,[18] whereas addition of an excess amount of methyl viologen slowly quenched the fluorescence of CF (Figure S7, Supporting Information). These results demonstrated the size-selective permeability of the nanocapsule shell: the shell of nanocapsule **3a** permits the passage of small molecules such as H_3O^+ or methyl viologen but not large molecules such as CF or Rh6G. The permeability of the nanocapsule shell is expected to be tuned by changing either the cross-linking density of the shell or the medium in which the nanocapsule is dispersed. Controlling the permeability of the nanocapsule by changing its dispersion media has been demonstrated recently.[13]

(16) Luna-Bárcenas, G.; Meredith, J. C.; Sanchez, I. C.; Johnston, K. P.; Gromov, D. G.; dePablo, J. J. *J. Chem. Phys.* **1997**, *107*, 10782–10792.
(17) Buschmann, H.-J.; Jansen, K.; Schollmeyer, E. *Thermochim. Acta* **1998**, *317*, 95.
(18) Dergunov, S. A.; Miksa, B.; Ganus, B.; Lindner, E.; Pinkhassik, E. *Chem. Commun.* **2010**, 1485–1487.

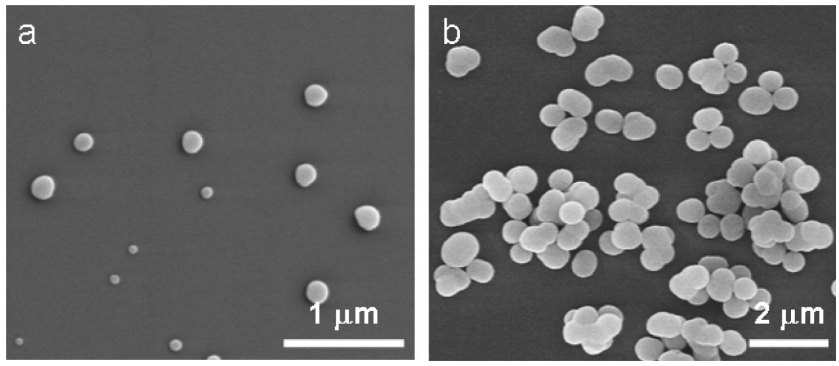

Figure 8. (a) SEM image of polymer nanocapsule **3a** prepared in acetonitrile (**1**:**2a** = 1:48). (b) SEM image of polymer nanocapsule **3a** prepared in chloroform (**1**:**2a** = 1:6).

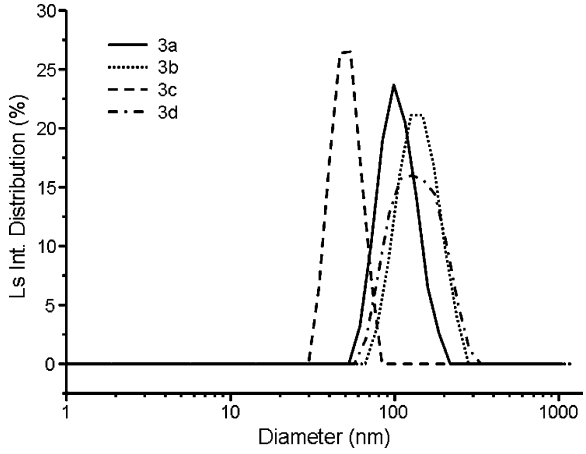

Figure 9. Size distribution of polymer nanocapsules **3a**−**d** synthesized from **1** and dithiols with different lengths (**2a**−**d**, respectively) (**1**:**2** = 1:48) (determined by DLS).

Probing and Modifying the Surface by Host−Guest Chemistry. One of the unique properties of the polymer capsules described here comes from the fact that they are made of a CB[6] derivative with a cavity, which can form exceptionally stable host−guest complexes with polyamines such as spermine or spermidine (binding constant $>10^9$ M^{-1}), which allowed us to probe and tailor their surface using host−guest chemistry, or noncovalent interactions between the accessible CB[6] units on the surface and polyamine derivatives.[10,19]

We first investigated how many molecular cavities constituting the shell of the nanocapsules are accessible using a fluorescent probe, fluorescein isothiocyanate (FITC)-tagged polyamine **4**, which forms a stable 1:1 complex with **1** (Figure S8, Supporting Information). After a dispersion of polymer nanocapsule **3a** in methanol was treated with the fluorescent probe (1.00 equiv with respect to the host molecules present in the nanocapsule), the mixture was dialyzed to quantify the amount of the probe molecule remaining unbound by fluorescence spectroscopy. It turned out that almost 85% of the host molecules **1** that constitute the polymer nanocapsule **3a** are accessible to the fluorescent probe, implying that the nanocapsule shell is only one or two monomers thick, which is parallel with the thickness of the nanocapsule (∼2 nm) measured by HR- and cryo-TEM studies.

The strong host−guest interaction ensures not only near-quantitative binding of the probe **4** to the surface of the nanocapsule (Figure S9a, Supporting Information) but also stability of the noncovalently modified surface, as a negligible amount of free **4** was released from the surface-decorated nanocapsule, even after prolonged dialysis (Figure S9b). Furthermore, this noncovalent surface modification little affects the shape and size of the polymer nanocapsule, as indicated by the SEM and TEM images of polymer nanocapsule **3a** decorated with **4** (Figure S10, Supporting Information).[7] Little change in the size distribution of polymer nanocapsule **3a** was also observed after the surface modification with **4**, as judged by DLS (Figure S11, Supporting Information).

As described above, nanocapsule **3a** prepared in chloroform is large enough to be observed by confocal laser scanning microscopy when a fluorescent dye is encapsulated inside the capsule or its surface is decorated with a fluorescent dye (Figure 10a). The confocal microscope images (Figure 10b) of polymer nanocapsule **3a** encapsulating Rh6G (Rh6G@**3a**), the surface of which had been decorated with **4**, showed green fluorescent circles corresponding to **4** on the surface of **3a**, which were overlapped with red fluorescent dots corresponding to Rh6G encapsulated inside the nanocapsule. These results confirmed that the surface of the polymer nanocapsule can be tailored via noncovalent interactions while guest molecules are being encapsulated in the interior. Almost any functional tags including targeting ligands and imaging probes, if they are attached to polyamines, can be introduced on the surface in a noncovalent, nondestructive, and modular manner, which makes the polymer nanocapsules potentially useful in many applications, including targeted delivery as briefly demonstrated in our previous communication.[7,8]

Other Monomers and Reactions Leading to Polymer Nanocapsules. The polymer nanocapsules made of CB[6] units have many interesting properties and application perspectives, and this synthetic approach is not limited to the specific monomer **1**. Polymer hollow spheres seem to be produced from almost any building blocks with a flat core and multiple polymerizable groups at the periphery, which can direct the polymer growth in lateral directions. For instance, photopolymerization of a triphenylene derivative containing six allyl groups with dithiol **2a** successfully produced a polymer nanocapsule with an average diameter of 900 ± 120 nm in acetonitrile, as described in our previous communication.[7] In addition, thermal thiol−ene click reaction between a zinc phthalocyanine derivative containing eight pentene groups and dithiol **2c** in the presence of a radical initiator such as 2,2′-azobisisobutyronitrile (AIBN) in ethanol/DMSO at 70 °C

(19) Lee, H.-K.; Park, K. M.; Jeon, Y. J.; Kim, D.; Oh, D. H.; Kim, H. S.; Park, C. G.; Kim, K. *J. Am. Chem. Soc.* **2005**, *127*, 5006–5007.

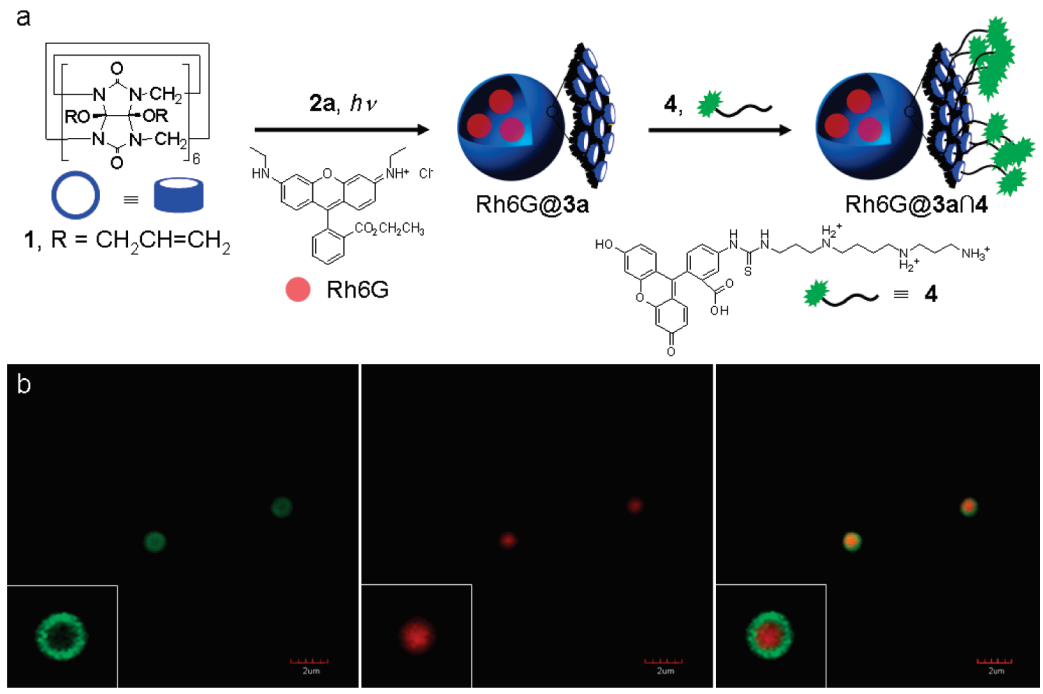

Figure 10. (a) Schematic illustration of encapsulation of dye molecules and noncovalent surface modification of the polymer nanocapsules. (b) Confocal microscope images of polymer nanocapsule **3a** encapsulating rhodamine 6G (Rh6G@**3a**) (prepared in chloroform), whose surface was decorated with **4** (scale bar = 2 μm). The confocal microscope images were obtained with a dispersion of the polymer nanocapsule in glycerol (left, FITC emission; center, rhodamine 6G emission; right, composite overlay of two channels; inset, enlarged images of the nanocapsules).

produced a polymer nanocapsule with an average diameter of 210 ± 70 nm, the details of which will be published separately.

Apparently, this synthetic approach is not limited to thiol−ene click reaction. Other reactions such as amide bond formation and olefin cross-metathesis reaction can be used to produce polymer nanocapsules. For example, reaction of a CB[6] derivative containing 12 terminal amine groups and an activated dicarboxylic acid produced a polymer nanocapsule with an average diameter of 70 ± 20 nm in chloroform/methanol in the presence of a catalytic amount of triethylamine. The direct synthetic approach based on the amide bond formation not only produced polymer nanocapsules but also allowed the incorporation of new functionalities such as disulfide bridges into polymer nanocapsules.[20] We are currently expanding this work to include other building blocks with different shapes and sizes and other reactions for the direct synthesis of polymer nanocapsules.

Self-Assembly of Polymer Nanocapsules through Irreversible Covalent Bond Formation. Although there are a number of examples of multicomponent assembly of nanostructures such as nanocages using reversible covalent chemistry,[21] including imine formation,[22] disulfide exchange,[23] and alkene metathesis,[24] the spontaneous formation of hollow spheres presented here is a rare example of self-assembly through irreversible covalent bond formation.[25] In general, it is extremely difficult to control the assembly of molecules in solution via irreversible covalent bond formation, as it tends to produce random macromolecular objects with 3D polymer networks. As we demonstrated here, however, molecular building blocks with a flat core and multiple polymerizable groups at the periphery can direct the polymer growth predominantly in lateral directions, leading to the formation of single-monomer-thick 2D oligomeric patches, which are key intermediates for the formation of the hollow spheres. Although the detailed mechanism remains to be elucidated, the conversion of 2D oligomeric intermediates into hollow spheres with radii larger than a critical value is thermodynamically favorable, as suggested by our theoretical model, which is also congruent with the rapid formation of the nanocapsules described above. This work suggests that the assembly of other nanostructures such as nanotubes[26] and tori may also be achieved through irreversible covalent bond formation once molecular building blocks are carefully designed.

Conclusions

We have presented a detailed study of the direct synthesis of polymer nanocapsules, which does not require any template, and core removal. Thiol−ene click reaction between a CB[6] derivative (**1**) with 12 allyloxy groups at the periphery and

(20) Kim, E.; Kim, D.; Jung, H.; Lee, J.; Paul, S.; Selvapalam, N.; Yang, Y.; Lim, N.; Park, C. G.; Kim, K. *Angew. Chem., Int. Ed.* **2010**, *49*, 4405–4408.
(21) Rowan, S. J.; Cantrill, S. J.; Cousins, G. R. L.; Sanders, J. K. M.; Stoddart, J. F. *Angew. Chem., Int. Ed.* **2002**, *41*, 898–952.
(22) (a) Liu, X.; Liu, Y.; Li, G.; Warmuth, R. *Angew. Chem., Int. Ed.* **2006**, *45*, 901–904. (b) Liu, Y.; Liu, X.; Warmuth, R. *Chem. Eur. J.* **2007**, *13*, 8953–8959. (c) Chichak, K. S.; Cantrill, S. J.; Pease, A. R.; Chiu, S.-H.; Cave, G. W. V.; Atwood, J. L.; Stoddart, J. F. *Science* **2004**, *304*, 1308–1312. (d) Hartley, C. S.; Elliott, E. L.; Moore, J. S. *J. Am. Chem. Soc.* **2007**, *129*, 4512–4513.
(23) (a) Otto, S.; Furlan, R. L. E.; Sanders, J. K. M. *J. Am. Chem. Soc.* **2000**, *122*, 12063–12064. (b) Otto, S.; Furlan, R. L. E.; Sanders, J. K. M. *Science* **2002**, *297*, 590–593. (c) West, K. R.; Bake, K. D.; Otto, S. *Org. Lett.* **2005**, *7*, 2615–2618.
(24) (a) Kilbinger, A. F. M.; Cantrill, S. J.; Waltman, A. W.; Day, M. W.; Grubbs, R. H. *Angew. Chem., Int. Ed.* **2003**, *42*, 3281–3285. (b) Trnka, T. M.; Grubbs, R. H. *Acc. Chem. Res.* **2001**, *34*, 18–29. (c) Zhang, W.; Moore, J. S. *J. Am. Chem. Soc.* **2005**, *127*, 11863–11870.
(25) Lindsey, J. S. *New J. Chem.* **1991**, *15*, 153–180.
(26) Spontaneous formation of cross-linked graphitic nanotubes triggered by olefin metathesis was reported, but the mechanism of the nanotube formation is unclear: Jin, W.; Fukushima, T.; Kosaka, A.; Niki, M.; Ishii, N.; Aida, T. *J. Am. Chem. Soc.* **2005**, *127*, 8284–8285.

dithiols directly produced polymer nanocapsules with a highly stable structure and relatively narrow size distribution. Based on a number of observations including the intermediates detected by DLS, TEM, and SEM studies, a mechanism for the nanocapsule formation was proposed, which includes 2D oligomeric patches turning into a hollow sphere. A theoretical study supports that the formation of a hollow sphere from a disk-shaped intermediate can be thermodynamically favorable under certain conditions. The effects of various factors such as reaction temperature, monomer concentration, and reaction medium on the formation of polymer nanocapsules have been investigated, which qualitatively agreed with those predicted by the theory. An interesting feature of the polymer nanocapsules was that the polymer shell made of a CB[6] derivative allows facile tailoring of its surface properties in a noncovalent and modular manner by virtue of the unique recognition properties of the accessible molecular cavities exposed on the surface. This approach appears to be applicable to any building unit with a flat core and multiple polymerizable groups at the periphery which can direct polymer growth in lateral directions. Other reactions, such as amide bond formation, can be used for the synthesis of polymer nanocapsules in this approach. This novel approach to polymer nanocapsules represents a rare example of irreversible covalent self-assembly and suggests that the assembly of nanometer-scale objects with desired structures, shape, and morphology can also be achieved through irreversible covalent bond formation with carefully designed molecular building blocks.

Experimental Section

Materials and General Methods. All the reagents and solvents employed were commercially available and used as supplied without further purification. $(Allyloxy)_{12}$cucurbit[6]uril (**1**),[10] $HS(CH_2CH_2O)_4CH_2CH_2SH$ (**2b**),[27] and FITC-spermine conjugate **4**[10] were synthesized according to the literature. Photoreaction was performed in a quartz tube by irradiating UV light at 38 °C using a Rayonet photochemical reactor (model RMR-600) equipped with four 254 nm lamps and four 300 nm lamps. All the NMR data were recorded on a Bruker DPX-300 or DRX500 spectrometer. Cross-polarization magic-angle sample spinning (CPMAS) ^{13}C NMR experiments were carried out on a Bruker DPX-300 NMR spectrometer operating at 300.13 MHz for ^1H and 75.47 MHz for ^{13}C with a 4 mm double-resonance broadband MAS probe at a spinning rate of 10 kHz. For cross-polarization experiments, $^1H-^{13}C$ contact time was 2.5 ms, the 90° pulse length was 4 μs on both channels, and the repeating time amounted to 5 s. UV−visible absorption spectra were recorded on a Hewlett-Packard 8453 diode array spectrophotometer. All fluorescence measurements were performed with 10 mm quartz cells on a Shimadzu RF-5301PC spectrofluorometer. Dialysis was performed using a Spectra/Por RC membrane (MWCO = 8000). FT-IR spectra were recorded on a Perkin-Elmer Spectrum GX FT-IR spectrophotometer. Dynamic and static light scattering experiments were performed on a DLS-7000 instrument (Otsuka Electronics) using an argon ion laser operating with vertically polarized light at $\lambda = 488$ nm. SEM images were collected using a Phillips XL30S FEG scanning electron microscope operating at 5 kV. High-resolution TEM images were recorded on a JEOL-2010F electron microscope operating at 200 kV. Cryo-TEM images were recorded on a Tecnai 12 electron microscope (Philips, Eindhoven, Netherlands) at approximately −170 °C and with a 120 kV acceleration voltage, equipped with a Multiscan 600 W CCD camera (Gatan, Inc., Warrendale, PA). Fluorescence images were observed on a Carl Zeiss LSM510 confocal laser scanning microscope.

Polymer Nanocapsules 3a. After being purged with N_2, a mixture of **1** (10.4 mg, 5.0 μmol) and dithiol **2a** (43.7 mg, 240 μmol) in methanol (10 mL) was irradiated with UV light (254 and 300 nm) in a photochemical reactor for 20 h. The product was purified by dialysis against methanol for 2 d to give a colloidal solution of polymer nanocapsule **3a** in methanol, which was usually used for further experiments. Removal of the solvent under a reduced pressure followed by drying under vacuum yielded polymer nanocapsule **3a** (20.5 mg; 87% based on **1**). Anal. Calcd for **3a** $[(C_{72}H_{96}N_{24}O_{24})_2(C_6H_{12}O_2S_2)_{31}(CH_4O)_6]_n$: C, 44.13; H, 6.48; N, 7.35; S, 21.74. Found: C, 44.25; H, 6.10; N, 7.03; S, 21.67. ^{13}C CP-MAS: δ = 155.8, 99.7, 74.3, 67.8, 60.6, 45.1, 34.6, 19.5. Since **1** is a limiting reactant in the polymerization reaction, the yield was calculated on the basis of the molar ratio of **1** initially used and **1** incorporated in the final product (**3a**), with the composition provided by elemental analysis. The FT-IR spectrum and solid-state ^{13}C NMR spectrum of **3a** are given in Figures S1 and S2 (Supporting Information), respectively.

Polymer Nanocapsule 3a′. Excess ethyl vinyl ether (505 mg, 7.0 mmol) was added to a dispersion of polymer nanocapsule **3a** (20.5 mg) in methanol (10 mL). After being purged with N_2, the mixture was irradiated with UV light (254 and 300 nm) for 20 h. The product was purified by dialysis against methanol for 2 d to obtain a colloidal solution of polymer nanocapsules **3a′**. Removal of most of the solvent followed by addition of diethyl ether yielded polymer nanocapsule **3a′** (13.8 mg, 81%). Anal. Calcd for **3a′** $[(C_{72}H_{96}N_{24}O_{24})(C_6H_{12}O_2S_2)_{7.4}(C_4H_9O_1)_{2.7}(CH_4O)_7(C_4H_{10}O)_4]_n$: C, 48.53; H, 7.39; N, 9.18; S, 12.88. Found: C, 48.15; H, 6.62; N, 8.79; S, 12.31.

Monitoring the Polymer Nanocapsule Formation. The photopolymerization of **1** and **2a** (1:48) in methanol was carried out in a cuvette with a cap following the above procedure. The reaction was monitored by DLS at various time points, such as 1, 2, 3, 4, 5, 30, 60, 180, 360, and 1200 min, to study the change in the hydrodynamic radius of the product. In a parallel experiment, the product was isolated at various time points of the reaction and characterized by FT-IR spectroscopy and elemental analysis. The reaction of **1** and **2a** (1:6) in chloroform was also monitored by DLS (Figure S4, Supporting Information) as described above. The product at each stage of the reaction was isolated and characterized by SEM and TEM.

Effect of Reaction Temperature. To study the effect of the reaction temperature on the formation of polymer nanocapsules, the photopolymerization of **1** and **2a** at various molar ratios was carried out on a benchtop and in a cold room (4 °C), where the temperatures inside the UV reactor were 38 and 8 °C, respectively. The average sizes of the polymer nanocapsule were measured by DLS studies.

Effect of Monomer Concentration. 1 and **2a** were photopolymerized with various concentrations of the reactants in methanol while keeping their ratio (1:48); the same procedure was followed for **3a**. The photoreaction was carried out with eight different concentrations of **1**: 5×10^{-3}, 3×10^{-3}, 1×10^{-3}, 5×10^{-4}, 3×10^{-4}, 1×10^{-4}, 8×10^{-5}, and 5×10^{-5} M. The average sizes of the polymer nanocapsule were measured by DLS studies.

Effect of Reaction Medium. The reaction between **1** and **2a** was carried out in acetonitrile (**1**:**2a** = 1:48) or chloroform (**1**:**2a** = 1:6) instead of methanol using the same procedure described above to produce polymer nanocapsule **3a**, the average diameter of which was measured by SEM.

Effect of the Length of Dithiol. A dispersion of polymer nanocapsules **3b−d** in methanol was synthesized using dithiols **2b−d** (**1**:dithiol =1:48), respectively, following the same procedure described for **3a**. The average diameters of the nanocapsules were determined by DLS studies.

Effect of Additives. α,ω-Dithiol **2a** (5.5 mg, 30 μmol) and 4-amino-1-butanol (446 μg, 5.0 μmol or 2.7 mg, 30 μmol, 1 or 6 equiv with respect to **1**, respectively) was added to a solution of **1** (10.4 mg, 5.0 μmol) in methanol (10 mL). After being purged with

(27) Huang, S.-T.; Kuo, H.-S.; Hsiao, C.-L.; Lin, Y.-L. *Bioinorg. Med. Chem.* **2002**, *10*, 1947–1952.

N_2, the mixture was irradiated with UV light (254 and 300 nm) for 20 h. The resulting dispersion was purified by dialysis for 2 d to give a colloidal solution of polymer nanocapsule **3a** in methanol. The average sizes of nanocapsules were determined by SEM.

Preparation of Dye-Encapsulating Polymer Nanocapsules (CF@3a and Rh6G@3a). After being purged with N_2, a mixture of **1** (10.4 mg, 5.0 μmol), **2a** (43.7 mg, 240 μmol), and carboxyfluorescein (3.80 mg, 10 μmol) in methanol (10 mL) was irradiated with UV light (254 and 300 nm) for 20 h. The resulting dispersion was purified by dialysis against methanol for 2 days to give a colloidal solution of CF-encapsulating polymer nanocapsule, CF@**3a**, in methanol. The resulting dispersion was used for fluorescence experiments. Similarly, rhodamine 6G (Rh6G)-encapsulating polymer nanocapsule, Rh6G@**3a**, was prepared by photoreaction of **1** (10.4 mg, 5.0 μmol), **2a** (5.5 mg, 30 μmol), and rhodamine 6G (4.80 mg, 10 μmol) in chloroform by following the same procedure.

Fluorescence Quenching Experiments To Study Permeability of Polymer Nanocapsules. The emission (536 nm) of CF encapsulated inside **3a** was monitored with two different excitation wavelengths (503 and 458 nm) simultaneously. A dispersion of CF-encapsulating polymer nanocapsule, CF@**3a**, in methanol (1 mL), prepared as described above, was diluted with methanol (1 mL) in a cuvette, and fluorescence intensities, I_{503} and I_{458}, as well as the intensity ratio, I_{503}/I_{458}, were recorded as a function of time. One hundred seconds later, aqueous HCl solution (100 μL, 0.5 M in water) or methyl viologen (MV^{2+}) solution (400 μL, 5.0 M in methanol) was added to the cuvette, and the intensity ratio, I_{503}/I_{458}, continued to be monitored (Figure S7, Supporting Information).

Determination of Accessible CB[6] Cavities on the Nanocapsule Surface. A dispersion of polymer nanocapsule **3a** (2.0 mg) in methanol (1 mL), which was prepared as described above, was treated with the FITC-spermine conjugate **4** (0.30 mg, 0.44 μmol; 1.0 equiv with respect to the amount (0.91 mg, 0.44 μmol) of the CB[6] host present in the nanocapsule, which was determined by elemental analysis), and the resulting dispersion was gently shaken for 12 h. Unbound **4** was then removed and collected by dialysis for 12 h. The amount of unbound **4** was measured by fluorometry. This experiment was repeated several times, and the average value of unbound **4** was 0.066 ± 0.02 μmol (0.15 ± 0.05 equiv), which indicated that ~85% of CB[6] constituting the polymer nanocapsules **3a** is accessible by the FITC-spermine conjugate **4**. When 0.75, 0.50, or 0.25 equiv (with respect to the amount of the CB[6] host present in the nanocapsule) of **4** was used to decorate the surface of **3a** by following the same procedure described above, a negligible amount (<5%) of unbound **4** was recovered (measured by fluorometry) upon dialysis (Figure S9a, Supporting Information).

Monitoring the Release of Free 4 from Nanocapsule 3a Decorated with 4. A dispersion of polymer nanocapsule **3a** decorated with **4** (1.0 equiv.) in methanol (5 mL) was prepared as described above. After the removal of unbound **4** by dialysis for 2 d, the dispersion of the surface-decorated nanocapsule was further subjected to dialysis against methanol (2 L) for 70 h,and the release of free **4** was monitored by fluorometry. A negligible amount (<3%) of **4** was found to be released during the dialysis (Figure S9b, Supporting Information).

Characterization of Surface-Modified Polymer Nanocapsules. A dispersion of polymer nanocapsule **3a** decorated with **4** (1.0 equiv) in methanol (5 mL) was prepared as described above. After the removal of unbound **4** by dialysis for 2 d, the resulting surface-modified polymer nanocapsule was characterized by SEM, TEM, DLS, UV−visible absorption, and emission spectroscopy (Figure S10 and S11, Supporting Information).

Surface Modification of the Rh6G-Encapsulating Polymer Nanocapsule Using 4. To the dispersion of Rh6G@**3a** in chloroform (5 mL) was added FITC-spermine conjugate **4** (1.5 mg, 2.2 μmol), and the resulting dispersion was gently shaken for 12 h. The unbound **4** was removed by dialysis against chloroform for 2 days to yield Rh6G-encapsulating polymer nanocapsule decorated with **4** (Rh6G@**3a**∩**4**), which was characterized by confocal microscopy.

Acknowledgment. D.K. and E.K. contributed equally to this work. We gratefully acknowledge the Creative Research Initiatives (K.K.), Brain Korea 21 (K.K. and W.S.), NCRC (W.S.), and World Class University (WCU) program (Project No. R31-2008-000-10059-0) (K.K.) of the Korean Ministry of Education, Science and Technology (MOEST) for support of this work. Thanks are also due to Prof. S. S. Han for cryo-TEM experiments.

Note Added in Proof. After submission of this paper, the direct transformation of graphene to fullerene, which is conceptually similar to the conversion of a 2D oligomeric patch into a nanocapsule as described here, was reported.[28]

Supporting Information Available: Further SEM and TEM images, DLS, and spectral characterization; complete ref 7. This material is available free of charge via the Internet at http://pubs.acs.org.

JA1039242

(28) Chuvilin, A.; Kaiser, U.; Bichoutskaia, E.; Besley, N. A.; Khlobystov, A. N. *Nat. Chem.* **2010**, *2*, 450–453.